Journal of Sound and Vibration (1999) **225**(3), 401–424
Article No. jsvi.1994.2200, available online at http://www.idealibrary.com on IDEAL®

THE DESIGN OF ACTIVE NOISE CONTROL SYSTEMS FOR COMPACT AND DISTRIBUTED SOURCES

M. O. TOKHI

Department of Automatic Control and Systems Engineering, The University of Sheffield, Mappin Street, Sheffield S1 3JD, England

(*Received* 24 *August* 1993, *and in final form* 5 *September* 1994)

This paper presents a coherent method of design of active noise control systems for compact and distributed sources of noise in a three-dimensional non-dispersive propagation medium. An analysis of single-input single-output, single-input multi-output and multi-input multi-output control structures is provided. Conditions for the robust operation of such systems on the basis of optimum cancellation, in relation to controller design, are determined. These conditions are interpreted as constraints on the geometric compositions of the system.

1. INTRODUCTION

Active noise control (ANC) is realized by artifically generating secondary (cancelling) source(s) of sound through detecting the primary (unwanted) noise and processing it by a suitable electronic controller, so that when the secondary wave is superimposed on the primary wave the two destructively interfere with one another and reduction of the unwanted sound occurs. Theoretical and practical investigations have shown that, generally, due to the broadband nature of the noise emitted by practical sources, the control process is required to realize suitable continuous frequency-dependent characteristics so that cancellation over a broad range of frequencies of the noise is achieved [1–4]. Moreover, in practice, the characteristics of sources of noise vary, e.g. due to operating conditions, leading to time-varying spectra. Furthermore, the characteristics of system components are subject to variation: e.g., due to ageing, environmental effects, etc. Therefore, the control process is further required to incorporate an adaptive capability so that the required performance is achieved and maintained. Through his experiments of reducing transformer noise, Conover was the first to realize the need for a "black-box" controller that would adjust the cancelling signal in accordance with information gathered at a remote distance from the transformer, as the performance of his ANC system was deteriorating from time to time due to the time-varying nature of the transformer noise [5, 6]. Later it has been realized by numerous researchers that for an ANC system to be practically successful it is essential that it incorporates an adaptive capability [1, 7–17].

0022-460X/99/330401 + 24 $30.00/0

In practice, sources of noise can broadly be classified as compact or distributed. A compact source of noise is theoretically modelled as a point source with contours of equal pressure levels forming spherical surfaces around the source. A distributed source of noise, on the other hand, can be modelled as a set of point sources distributed around the surface of the source. In cancelling the noise of a compact source, a single detector is generally sufficient to obtain the required signal information needed to generate the cancelling signal. This leads to the realization of a control structure incorporating a single-input signal. However, in cancelling the noise of a distributed source, to obtain sufficient signal information, a multiple set of detectors will be required. This will lead to the realization of a multi-input control structure. Similarly, at the output end, the performance requirements of the system as related to the physical extent of cancellation in the medium, will lead to the realization of either single-output or multi-output control structures. Therefore, depending on the application a suitable control structure incorporating the required number of inputs and outputs can be employed.

The analysis presented in this paper is concerned with the cancellation of noise of both compact and distributed sources in three-dimensional (free-field) propagation. The system is considered within the realization structures of the single-input single-output (SISO), single-input multi-output (SIMO) and multi-input multi-output (MIMO) forms. The controller design relations are developed in the frequency domain. These can, equivalently, be thought of either in the complex frequency s-domain or the z-domain allowing the practical realization of the corresponding controller in either the continuous time or the discrete time using analogue or digital techniques accordingly.

The analysis is focused on ANC systems in stationary (steady-state) conditions. This corresponds to a system with fixed controller of the required characteristics under situations where substantial variations in the characteristics of secondary source(s), transducers and other electronic equipment used do not occur. In an adaptive ANC system, this means that once a steady state (stationary) condition has reached the situation is equivalent to the case of the fixed controller. Therefore, in an adaptive ANC system the analysis applies to periods of time when a steady state condition has reached and substantial variation in the parameter values do not occur.

2. ACTIVE NOISE CONTROL STRUCTURE

A schematic diagram of a general ANC structure, namely the MIMO feedforward control structure (FFCS), is shown in Figure 1(a). A set of n primary point sources emit unwanted acoustic signals (noise) into the medium. This is detected by a set of n detectors, processed by the controller and fed to a set of k secondary sources. The secondary signals thus generated are superimposed upon the unwanted noise so that the noise level is reduced at a set of k observation points. The corresponding frequency-domain equivalent block diagram of Figure 1(a) is shown in Figure 1(b) where $\mathbf{E}$ is an $n \times n$ matrix representing transfer characteristics of the acoustic paths between the primary sources and the detectors, $\mathbf{F}$ is a $k \times n$

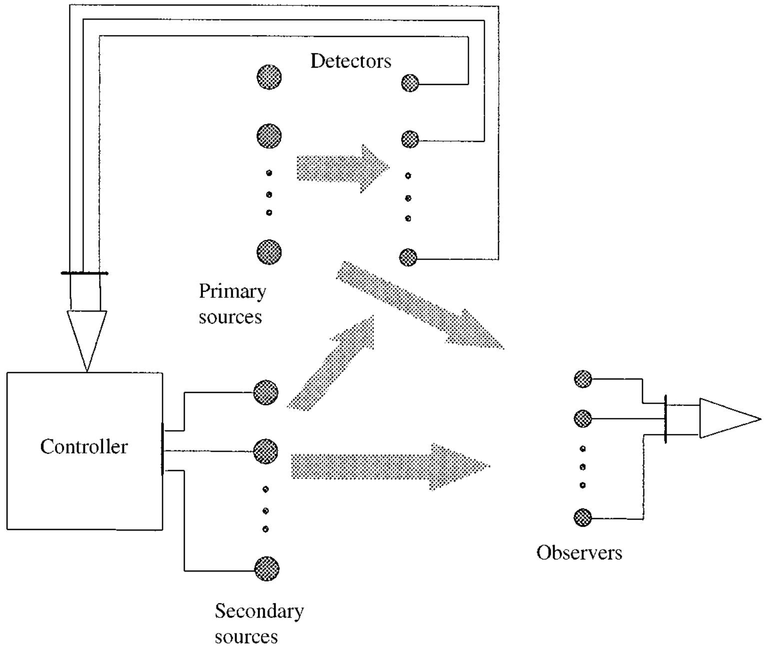

(a)

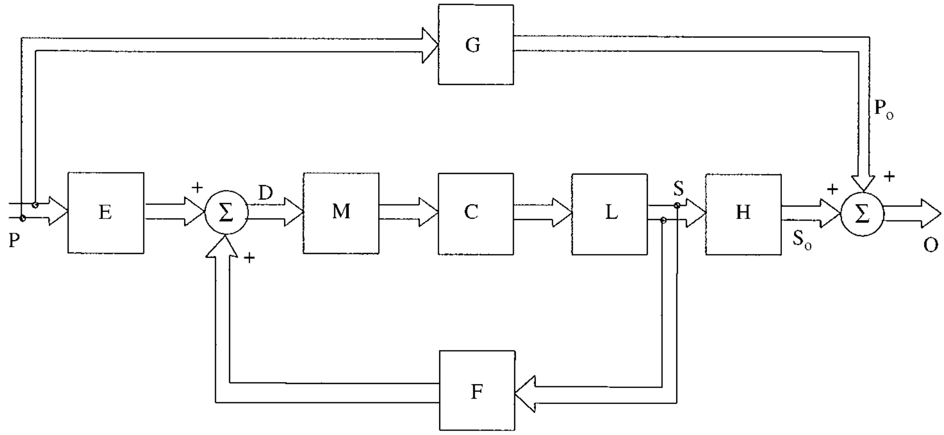

(b)

Figure 1. Active noise control structure: (a) Schematic diagram. (b) Block diagram.

matrix representing transfer characteristics of the acoustic paths between the secondary sources and the detectors, $\mathbf{G}$ is an $n \times k$ matrix representing transfer characteristics of the acoustic paths between the primary sources and the observers, $\mathbf{H}$ is a $k \times k$ matrix representing transfer characteristics of the acoustic paths between the secondary sources and the observers, $\mathbf{M}$ is an $n \times n$ diagonal matrix representing transfer characteristics of the detectors, $\mathbf{P}$ is a $1 \times n$ matrix representing the primary signals at the source points, $\mathbf{P}_o$ is a $1 \times k$ matrix representing the primary signals at the observation points, $\mathbf{S}$ is a $1 \times k$ matrix representing the secondary signals at the source points, $\mathbf{S}_o$ is a $1 \times k$ matrix representing the secondary signals at the observation points, $\mathbf{D}$ is a $1 \times n$ matrix representing the detected signals, and $\mathbf{O}$ is a $1 \times k$ matrix representing the combined primary and secondary signals at the observation points.

As seen in Figure 1(a), each detector gives a combined measure of the primary and secondary waves that reach the corresponding detection point. The secondary waves thus reaching the detectors form closed feedback loops that can cause the system to become unstable. Therefore, a careful consideration of these loops is necessary at a design stage. Alternative techniques attempting to avoid the instability problem in one-dimensional propagation (duct noise) by isolating the detector from secondary source radiation through using either unidirectional detectors or multiple-detector/multiple-source configurations such as acoustic dipole and tripole have been reported [18–22]. It is possible to avoid the instability problem in three-dimensional propagation by using unidirectional detector(s) or by employing indirect detection [23]. However, a stability analysis of the system based on relative stability measures will lead to a robust design [24].

Note, in Figure 1, that moving the observation points so that to coincide with the detection points will lead to a feedback control structure (FBCS). This type of structure has been investigated for the SISO system extensively [23, 25–34]. The feedforward control structure, on the other hand, has more popularly been employed and investigated, as a general structure, in one-dimensional as well as three-dimensional enclosed and free fields [1, 4–6, 15–17, 23–26, 35–39].

3. DESIGN OF THE CONTROLLER

The objective in Figure 1 is to reduce the level of noise to zero at the observation points. This corresponds to the minimum variance design criterion in a stochastic environment. This requires the observed primary and secondary signals at each observation point to be equal in magnitudes and have a phase difference of 180°:

$$\mathbf{S}_o = -\mathbf{P}_o. \tag{1}$$

By using the block diagram in Figure 1(b), P_o and S_o can be expressed as

$$\mathbf{P}_o = \mathbf{PG}, \qquad \mathbf{S}_o = \mathbf{PEMCL}[\mathbf{I} - \mathbf{FMCL}]^{-1}\mathbf{H}, \tag{2}$$

where $\mathbf{I}$ is the identity matrix. Substituting for $\mathbf{P}_o$ and $\mathbf{S}_o$ from equation (2) into equation (1) and simplifying yields the required controller transfer function as

$$\mathbf{C} = \mathbf{M}^{-1}\mathit{\Delta}^{-1}\mathbf{GH}^{-1}\mathbf{L}^{-1}, \tag{3}$$

where $\mathit{\Delta}$ is an $n \times n$ matrix given by

$$\mathit{\Delta} = \mathbf{GH}^{-1}\mathbf{F} - \mathbf{E}. \tag{4}$$

Equation (3) represents the required controller design relation for optimum cancellation of noise at the observation points. In designing such a controller a careful consideration of the acoustic feedback loops, due to secondary source radiation reaching the detectors, that can cause the system to become unstable is required. Moreover, note in equation (3) that, for given sources, sensors and necessary electronics, the controller characteristics are dependent on the transfer characteristics of the acoustic paths and, hence, system geometry. A study of this dependence will give an insight into the complexity and practical realization aspects of the controller and, therefore, is extremely important in a design stage.

Note in Figure 1 that the control structure utilized includes the same number of secondary sources as the observation points. Similarly, the number of detectors is equal to the number of the primary sources. These are required for optimum cancellation of noise to be achievable at the observation points. This is evidenced in the corresponding design relation for the required controller in equation (3), requiring inversion of **H** and Δ, for which both **E** and **H** have to be square matrices. This implies that a control structure in which the number of secondary sources is not equal to the number of observation points and/or the number of detectors is not equal to the number of primary sources will lead to a sub-optimal design with which full cancellation of noise at the observation points will not be achievable. For a practically acceptable level of performance to be achieved with such a structure, the controller design can be based on minimization of some function of the noise, e.g. in a least-squares sense, at the observation points.

4. LIMITATIONS IN CONTROLLER DESIGN

It follows from equation (3) that for given detectors and secondary sources with necessary electronic components, the controller characteristics required for optimum cancellation are dependent on the characteristics of the acoustic paths from the primary and secondary sources to the detection and observation points. Any set of such points in the medium requires particular controller characteristics. In particular, if the set of detection and observation points are such that the determinant of Δ in equation (3) becomes zero then the critical situation of infinite-gain controller (IGC) requirement arises. The locus of such points in the medium (as a practical limitation in the design of the controller) is, therefore, of crucial interest.

Under the situation of the IGC requirement, equation (4), for periodic waves, can be written as

$$|\Delta(\mathrm{j}\omega)| = |\mathbf{G}(\mathrm{j}\omega)\mathbf{H}^{-1}(\mathrm{j}\omega)\mathbf{F}(\mathrm{j}\omega) - \mathbf{E}(\mathrm{j}\omega)| = 0, \tag{5}$$

where $\mathbf{E}(\mathrm{j}\omega)$, $\mathbf{F}(\mathrm{j}\omega)$, $\mathbf{G}(\mathrm{j}\omega)$ and $\mathbf{H}(\mathrm{j}\omega)$ represent the frequency responses of the corresponding acoustic paths in Figure 1, j is the unit imaginary number and ω is radian frequency. Note that equation (5) is given in terms of the characteristics of the acoustic paths in the system. This implies that the IGC requirement is a geometry-related problem in an ANC system. Therefore, an analysis of equation (5) will lead to the identification of loci of (detection and observation) points in the medium for which the IGC requirement holds. To obtain the solution of equation (5) an SISO system is considered first. The results obtained are then used and extended to the SIMO and MIMO ANC systems.

4.1. SINGLE-INPUT SINGLE-OUTPUT SYSTEM

Let the ANC system in Figure 1 incorporate a single primary source ($n = 1$) and a single secondary source ($k = 1$) and the functions $\mathbf{E}(j\omega)$, $\mathbf{F}(j\omega)$, $\mathbf{G}(j\omega)$ and $\mathbf{H}(j\omega)$, in this case, be denoted by $\mathbf{e}(j\omega)$, $\mathbf{f}(j\omega)$, $\mathbf{g}(j\omega)$ and $\mathbf{h}(j\omega)$ with the associated distances as r_e, r_f, r_g and r_h respectively:

$$\mathbf{E}(j\omega) = \mathbf{e}(j\omega) = \frac{A}{r_e}\,e^{-j(\omega/c)r_e}, \quad \mathbf{F}(j\omega) = \mathbf{f}(j\omega) = \frac{A}{r_f}\,e^{-j(\omega/c)r_f}$$

$$k = n = 1,$$

$$\mathbf{G}(j\omega) = \mathbf{g}(j\omega) = \frac{A}{r_g}\,e^{-j(\omega/c)r_g}, \qquad \mathbf{H}(j\omega) = \mathbf{h}(j\omega) = \frac{A}{r_h}\,e^{-j(\omega/c)r_h} \tag{6}$$

where A is a constant. Substituting for $\mathbf{E}(j\omega)$, $\mathbf{F}(j\omega)$, $\mathbf{G}(j\omega)$ and $\mathbf{H}(j\omega)$ from equation (6) into equation (5) and simplifying yields

$$\left(\frac{r_e}{r_e}\right) e^{-j(r_f - r_e)\,\omega/c} = \left(\frac{r_g}{r_h}\right) e^{-j(r_g - r_h)\,\omega/c}.$$

This equation is true if and only if the amplitudes as well as the exponents (phases) on either side of the equation are equal. Equating the amplitudes and the phases, accordingly, yields

$$r_e/r_f = r_g/r_h = a, \quad r_f - r_e = r_h - r_g, \tag{7}$$

where a is a positive real number representing the distance ratio. Equation (7) defines the locus of points for which $|\Delta(j\omega)| = 0$ and, for optimum cancellation to be achieved at the observation point, the controller is required to have an infinitely large gain. Note that this equation is in terms of the distances r_e, r_f, r_g and r_h only. Therefore, the critical situation of IGC requirement is determined only by the locations of the detector and observer relative to the primary and secondary sources.

Eliminating r_f and r_h in equation (7) and simplifying yields

$$r_e(a - 1) = r_g(a - 1). \tag{8}$$

Two possible situations, namely $a = 1$ and $a \neq 1$, are considered separately.

4.1.1. *Unity distance ratio*

For a unity distance ratio equation (8) yields the identity $0 = 0$. Therefore, substituting for $a = 1$ into equation (7) yields the locus of points for IGC requirement as

$$r_e/r_f = 1 \quad \text{and} \quad r_g/r_h = 1. \tag{9}$$

If the locations of the primary and secondary sources are fixed then each relation in equation (9) defines a plane surface perpendicularly bisecting the line joining the locations of the primary and secondary sources (see the Appendix A). This plane for the primary and secondary sources located at points $P(0, 0, 0)$ and $S(u_s, v_s, w_s)$

respectively with a distance r apart in a three-dimensional UVW-space is given by

$$\frac{u}{(r^2/2u_s)} + \frac{v}{(r^2/2v_s)} + \frac{w}{(r^2/2w_s)} = 1,$$

which intersects the $U-$, $V-$ and $W-$ axes at points $(r^2/2u_s, 0, 0)$, $(0, r^2/2v_s, 0)$ and $(0, 0, r^2/2w_s)$ respectively. If the detector is placed at any point on this plane (the IGC plane) and if at the same time the observer location coincides with a point on this plane then the "critical situation" of equation (5) occurs and the controller is required to have an infinitely large gain for optimum cancellation to be achieved at the observation point,

4.1.2. *Non-unity distance ratio*

For a non-unity distance ratio, equations (7) and (8) yield

$$r_e/r_f = a, \quad r_g/r_h = a \quad \text{and} \quad r_e/r_g = 1. \tag{10}$$

It follows from Appendix A that each of the first two relations in equations (10) describe spherical surfaces. These surfaces for the primary and secondary sources located respectively at $P(0, 0, 0)$ and $S(u_s, v_s, w_s)$ are defined by

$$\left[u + \frac{a^2 u_s}{1-a^2}\right]^2 + \left[v + \frac{a^2 v_s}{1-a^2}\right]^2 + \left[w + \frac{a^2 w_s}{1-a^2}\right]^2 = \left[\frac{ar}{1-a^2}\right]^2, \quad a \neq 1, \tag{11}$$

which has a radius $R = ar/[1-a^2]$ and centre along the line PS at point $Q(-a^2u_s/(1-a^2), -a^2v_s/(1-a^2), a^2w_s/(1-a^2))$.

The third relation in equations (10) requires the equality of the distances r_e and r_g. The locus of such points in the three-dimensional UVW-space (for, say, constant r_e) is a sphere with radius equal to r_e and centre at the location of the primary source:

$$u^2 + v^2 + w^2 = r_e^2. \tag{12}$$

Therefore, the locus of points defined by equation (10) is given by intersection of the two spheres in equations (11) and (12). Such an intersection results a circle (the IGC circle) located in a plane that is at right angles with the line joining the centres of the spheres. The centre of the circle is the point of intersection of the plane and the line.

Manipulating equations (11) and (12) yields the plane of the IGC circle as

$$\frac{u}{(B/u_s)} + \frac{v}{(B/v_s)} + \frac{w}{(B/w_s)} = 1, \tag{13}$$

where

$$B = \frac{1}{2}\left[r^2 - \left(\frac{1}{a^2} - 1\right) r_e^2\right] = \frac{1}{2}\,[r^2 - (r_f^2 - r_e^2].\tag{14}$$

Equation (13) defines a plane surface on which the IGC circle is residing. It can be shown (see the Appendix A) that the line PS is at right angles with the plane of the IGC circle. This is shown in two dimensions in Figure 2(a) where point E is the

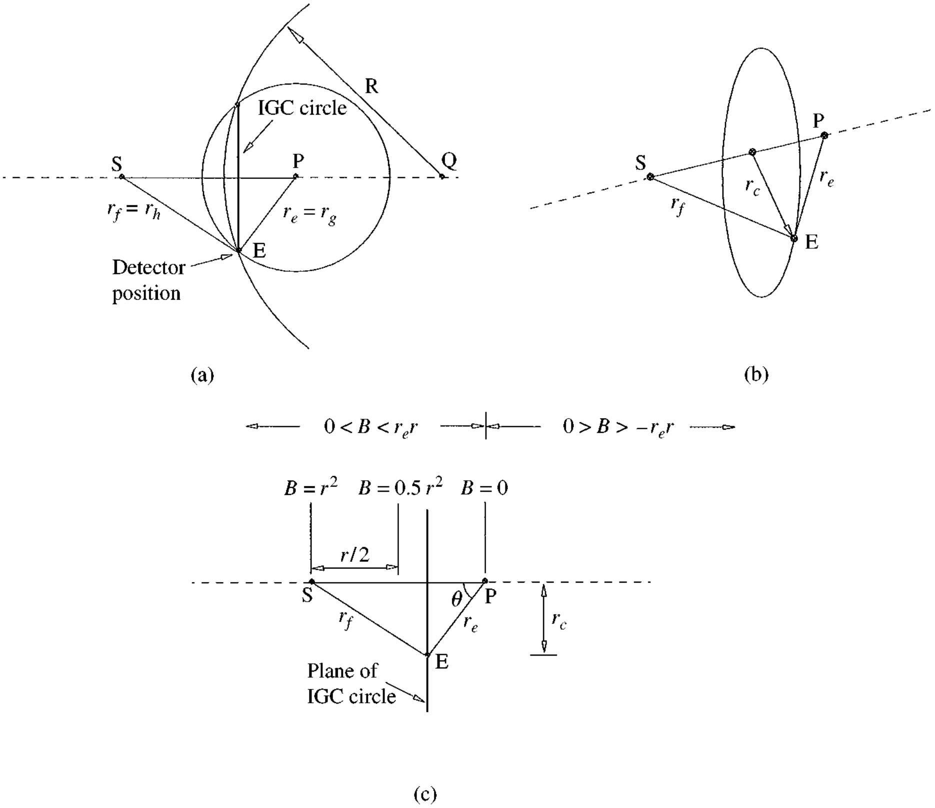

Figure 2. The infinite-gain controller system: (a) Formation, (b) IGC circle, (c) Position with detector location.

location of the detector. The corresponding IGC circle is shown in Figure 2(b) where r_c is the radius of the IGC circle.

The quantity B in equation (14) gives a measure of the intersection of the plane in equation (13) with the co-ordinate axes and, thereby, with the line PS. It is evident from equation (14) that B is dependent on r, r_e and r_f or, for constant r, is dependent on the location of the detector only. If θ denotes the angle between the lines PE and PS in a plane formed by these lines, see Figure 2(c), then the following holds:

$$r_f^2 = r^2 + r_e^2 - 2r_e r \cos\theta. \tag{15}$$

Substituting for r_f^2 from equation (15) into equation (14) yields

$$B = rr_e \cos\theta.$$

Therefore, as the detection point varies the limits for B are found to be

$$|B| < r_e r.$$

This variation, in relation to the location of the plane of the IGC circle, is shown in two dimensions in Figure 2(c).

The radius r_c of the IGC circle from Figure 2(c) is

$$r_c = r_e \sin\theta, \quad 0 \leqslant \theta \leqslant \pi.$$

Thus, the maximum value $r_{c\max}$ of the radius is r_e and occurs when the plane of the IGC circle intersects the line *PS* at point *P*, Figure 2(c). Movement of the plane to either side of point *P* will lead to a decrease in the radius. At the extreme cases where the line *PE* is aligned with the line *PS* (θ is either 0° or 180°) the radius r_c is zero. In general, for constant values of the angle θ the radius r_c is directly proportional to the distance r_e between the primary source and the detector. This implies that for r_c to be minimized the detector is required to be placed as close to the primary source as possible.

It follows from the above that the requirement of an infinitely large gain controller is directly linked with the locations of the detector and observer relative to the primary and secondary sources. This derives from the dependence of the controller characteristics on the transfer characteristics of the acoustic paths from the detector and observer to the primary and secondary sources which demand a particular controller transfer function for a particular set of detection and observation points in the medium. The above analysis reveals that particular sets of detection and observation points in the medium exist that for optimum cancellation require the controller to have an infinitely large gain. These form the locus of IGC requirement as follows.

(a) If the detector and observer are equidistant from the sources the locus is a plane surface that perpendicularly bisects the line joining the locations of the primary and secondary sources.

(b) If the detector and observer are not equidistant from the sources the locus is a circle, with centre along the line *PS* joining the locations of the primary and secondary sources, and on a plane that is parallel with that in (a). The radius of the circle is given by the distance between the detector and the line *PS*.

Note that, if the first two relations in equation (10) are divided side-by-side (upon assuming $a \neq 0$) then the following equivalent relations are obtained:

$$r_e/r_g = 1 \quad \text{and} \quad r_f/r_h = 1. \tag{16}$$

This means that starting with equation (16), rather than equation (10), will also lead to exactly the same results obtained in the preceding paragraphs.

Note in Figure 1(a) that if the observer and the detector coincide with one another then the FBCS is obtained. In such a process the distances r_g and r_h effectively become equal to the distances r_e and r_f, respectively. This in terms of the transfer functions **E**, **F**, **G** and **H** and the distances r_e, r_f, r_g and r_h corresponds to

$$r_g = r_e \quad \text{or} \quad \mathbf{G} = \mathbf{E}, \qquad r_h = r_f \quad \text{or} \quad \mathbf{H} = \mathbf{F}. \tag{17}$$

Projecting the above into the controller design relation in equation (3) yields, the corresponding controller design relation for the FBCS.

Substituting for **G** and **H** from equation (17) into equation (4) and simplifying yields $|\varDelta| = 0$ corresponding to the critical situation of the IGC requirement

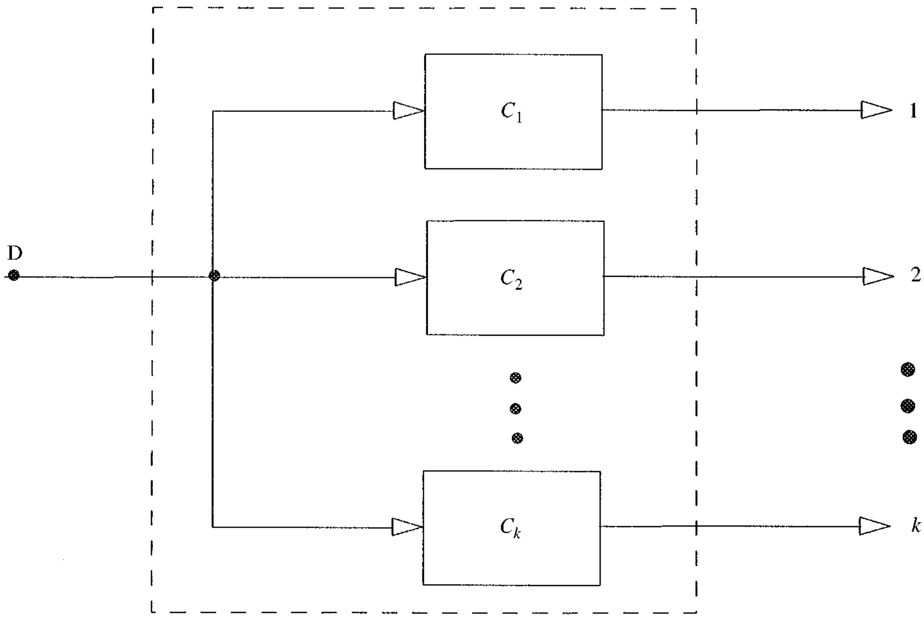

Figure 3. SIMO controller.

discussed above. Therefore, for optimum cancellation of noise, the FBCS will always require a controller with an infinitely large gain. With a practically acceptable compromise between system performance and controller gain, and careful consideration of system stability, reasonable amounts of cancellation of the noise can be achieved with this structure.

4.2. SINGLE-INPUT MULTI-OUTPUT SYSTEM

Let the ANC system in Figure 1 incorporate a single primary source ($n = 1$) and k secondary sources. Thus, the controller transfer characteristics, $\mathbf{C}$, in equation (3) will represent a $1 \times k$ matrix,

$$\mathbf{C} = [\mathbf{c}_1 \;\; \mathbf{c}_2 \;\; \cdots \;\; \mathbf{c}_k],$$

where $\mathbf{c}_i$ ($i = 1, 2, \ldots, k$) represents the required controller transfer function along the secondary path from the detector to secondary source i. In this manner, the controller is realized in an SIMO form as shown in Figure 3.

For reasons of simplicity, consider the case of $k = 2$ with the functions $\mathbf{E}(j\omega)$, $\mathbf{F}(j\omega)$, $\mathbf{G}(j\omega)$ and $\mathbf{H}(j\omega)$ represented as

$$\mathbf{E}(j\omega) = \mathbf{e}(j\omega), \quad \mathbf{F}(j\omega) = [\mathbf{f}_1(j\omega) \quad \mathbf{f}_2(j\omega)]^{\mathrm{T}},$$

$$\mathbf{G}(j\omega) = [\mathbf{g}_1(j\omega) \quad \mathbf{g}_2(j\omega)], \quad \mathbf{H}(j\omega) = \begin{bmatrix} \mathbf{h}_{11}(j\omega) & \mathbf{h}_{12}(j\omega) \\ \mathbf{h}_{21}(j\omega) & \mathbf{h}_{22}(j\omega) \end{bmatrix}, \tag{18}$$

where

$$\mathbf{e}(\mathrm{j}\omega) = \frac{A}{r_e}\,\mathrm{e}^{-\mathrm{j}(\omega/c)r_e}, \quad \mathbf{f}_i(\mathrm{j}\omega) = \frac{A}{r_{fi}}\,\mathrm{e}^{-\mathrm{j}(\omega/c)_{fi}}, \quad \mathbf{g}_i(\mathrm{j}\omega) = \frac{A}{r_{gi}}\,\mathrm{e}^{-\mathrm{j}(\omega/c)r_{gi}},$$

$$\mathbf{h}_{im}(\mathrm{j}\omega) = \frac{A}{r_{him}}\,\mathrm{e}^{-\mathrm{j}(\omega/c)r_{him}}, \tag{19}$$

$i = 1, 2$, $m = 1, 2$, A is a constant and r_e, r_{fi}, r_{gi} and r_{him} are the distances of the acoustic paths with transfer characteristics $\mathbf{e}(\mathrm{j}\omega)$, $\mathbf{f}_i(\mathrm{j}\omega)$, $\mathbf{g}_i(\mathrm{j}\omega)$ and $\mathbf{h}_{im}(\mathrm{j}\omega)$ respectively. Substituting for $\mathbf{E}(\mathrm{j}\omega)$, $\mathbf{F}(\mathrm{j}\omega)$, $\mathbf{G}(\mathrm{j}\omega)$ and $\mathbf{H}(\mathrm{j}\omega)$ from equations (18) into equation (5) and simplifying yields

$$\mathbf{f}_1(\mathbf{g}_1\mathbf{h}_{22} - \mathbf{g}_2\mathbf{h}_{21}) + \mathbf{f}_2(\mathbf{g}_2\mathbf{h}_{11} - \mathbf{g}_1\mathbf{h}_{12}) = \mathbf{e}(\mathbf{h}_{11}\mathbf{h}_{22} - \mathbf{h}_{21}\mathbf{h}_{12}). \tag{20}$$

Manipulating equation (20) yields the set of solutions

$$\frac{\mathbf{f}_1}{\mathbf{e}} = \frac{\mathbf{h}_{11}}{\mathbf{g}_1} = \frac{\mathbf{h}_{12}}{\mathbf{g}_2}, \quad \frac{\mathbf{f}_2}{\mathbf{e}} = \frac{\mathbf{h}_{21}}{\mathbf{g}_1} = \frac{\mathbf{h}_{22}}{\mathbf{g}_2}, \quad \frac{\mathbf{f}_2}{\mathbf{f}_1} = \frac{\mathbf{h}_{21}}{\mathbf{h}_{11}} = \frac{\mathbf{h}_{22}}{\mathbf{h}_{12}}. \tag{21}$$

Substituting for $\mathbf{e}$, $\mathbf{f}_1$, $\mathbf{f}_2$, $\mathbf{g}_1$, $\mathbf{g}_2$, $\mathbf{h}_{11}$, $\mathbf{h}_{12}$, $\mathbf{h}_{21}$ and $\mathbf{h}_{22}$ from equation (19) into equation (21) accordingly and simplifying yields

$$\left(\frac{r_e}{r_{f1}}\right)\mathrm{e}^{-\mathrm{j}(\omega/c)(r_{f1}-r_e)} = \left(\frac{r_{g1}}{r_{h11}}\right)\mathrm{e}^{-\mathrm{j}(\omega/c)(r_{h11}-r_{g1})} = \left(\frac{r_{g2}}{r_{h12}}\right)\mathrm{e}^{-\mathrm{j}(\omega/c)(r_{h12}-r_{g2})},$$

$$\left(\frac{r_e}{r_{f2}}\right)\mathrm{e}^{-\mathrm{j}(\omega/c)(r_{f2}-r_e)} = \left(\frac{r_{g1}}{r_{h21}}\right)\mathrm{e}^{-\mathrm{j}(\omega/c)(r_{h11}-r_{g1})} = \left(\frac{r_{g2}}{r_{h22}}\right)\mathrm{e}^{-\mathrm{j}(\omega/c)(r_{h22}-r_{g2})},$$

$$\left(\frac{r_{f1}}{r_{f2}}\right)\mathrm{e}^{-\mathrm{j}(\omega/c)(r_{f2}-r_{f1})} = \left(\frac{r_{h11}}{r_{h21}}\right)\mathrm{e}^{-\mathrm{j}(\omega/c)(r_{h21}-r_{h11})} = \left(\frac{r_{h12}}{r_{h22}}\right)\mathrm{e}^{-\mathrm{j}(\omega/c)(r_{h22}-r_{h12})}. \tag{22}$$

For the relations in equations (22) to hold, the amplitudes and phases on either side should be equal in each relation. Equating the amplitudes and phases accordingly yield

$$\frac{r_e}{r_{f1}} = \frac{r_{g1}}{r_{h11}} = \frac{r_{g2}}{r_{h12}} = a_1, \quad r_{f1} - r_e = r_{h11} - r_{g1} = r_{h12} - r_{g2},$$

$$\frac{r_e}{r_{f2}} = \frac{r_{g1}}{r_{h21}} = \frac{r_{g2}}{r_{h22}} = a_2, \quad r_{f2} - r_e = r_{h21} - r_{g1} = r_{h22} - r_{g2},$$

$$\frac{r_{f1}}{r_{f2}} = \frac{r_{h11}}{r_{h21}} = \frac{r_{h12}}{r_{h22}} = a_{12}, \quad r_{f2} - r_{f1} = r_{h21} - r_{h11} = r_{h22} - r_{h12}, \tag{23}$$

where a_1, a_2 and a_{12} are positive real numbers representing distance ratios. Equations (23) define loci of detection and observation points for which $|\Delta(\mathrm{j}\omega) = 0$ and the controller in each secondary path is required to have an infinitely large gain for optimum cancellation of noise to be achieved at the observation points.

The first relation in equations (23) describes the locations of the detection and observation points relative to the primary source and secondary source one (say). In this manner, this defines the locus of detection and observation points relative to the locations of the two sources, considered as fixed points in the medium. Using a similar analysis procedure as presented in the previous section with the SISO system reveals that for a unity distance ratio ($a_1 = 1$) the locus is given by

$$r_e/r_{f1} = r_{g1}/r_{h11} = r_{g2}/r_{h12} = 1. \tag{24}$$

Equations (24) define a plane surface that perpendicularly bisects the line joining the locations of the two sources (see Appendix A). The plane for the primary source and secondary source, located at $P(0, 0, 0)$ and $S_1(u_{s1}, v_{s1}, w_{s1})$ respectively with a distance r_1 apart in a three-dimensional UVW-space, is given by

$$\frac{u}{(r_1^2/2u_{s1})} + \frac{v}{(r_1^2/2v_{s1})} + \frac{w}{(r_1^2/2w_{s1})} = 1,$$

which intersects the $U-$, $V-$ and $W-$ axes at points $(r_1^2/2u_{s1}, 0, 0)$, $(0, r_1^2/2v_{s1}, 0)$ and $(0, 0, r_1^2/2w_{s1})$ respectively. If the locations of the detector as well as observers coincide with points on this plane then the critical situation of the IGC requirement arises.

If the distance ratio a_1 is not unity, then the first relation in equation (23) yields

$$r_e/r_{f1} = r_{g1}/r_{h11} = r_{g2}/r_{h12} = a_1 \quad \text{and} \quad r_e/r_{g1} = r_e/r_{g2} = r_{g1}/r_{g2} = 1. \tag{25}$$

It follows from Appendix A that both relations in equation (25) define spherical surfaces. The first relation defines the sphere

$$\left[u + \frac{a_1^2 u_{s1}}{1 - a_1^2}\right]^2 + \left[v + \frac{a_1^2 v_{s1}}{1 - a_1^2}\right]^2 + \left[w + \frac{a_1^2 w_{s1}}{1 - a_1^2}\right]^2 = \left[\frac{a_1 r_1}{1 - a_1^2}\right]^2, \quad a_1 \neq 1, \tag{26}$$

which has a radius $R_1 = a_1 r_1/|1 - a_1^2|$ and centre along the line PS_1 at point $Q_1(-a_1^2 u_{s1}/(1 - a_1^2), -a_1^2 v_{s1}/(1 - a_1^2), -a_1^2 w_{s1}/(1 - a_1^2))$. The second relation in equations (25) (for, say, constant r_e) defines a sphere with a radius equal to r_e and centre at the location of the primary source:

$$u^2 + v^2 + w^2 = r_e^2. \tag{27}$$

Therefore, the locus of detection and observation points defined by equations (25) is given by the intersection of the two spheres in equations (26) and (27). Such an intersection results in a circle located in a plane that is at right angles with the line passing through the centres of the spheres. The centre of the circle is the point of intersection of the plane and the line. Manipulating equations (26) and (27) yields this plane as

$$\frac{u}{(B_1/u_{s1})} + \frac{v}{(B_1/v_{s1})} + \frac{w}{(B_1/w_{s1})} = 1, \tag{28}$$

where $B_1 = \frac{1}{2}[r_1^2 - ((1 - a_1^2)/a_1^2) r_e^2] = \frac{1}{2}[r_1^2 - (r_{f1}^2 - r_e^2)]$. The point of intersection of the plane in equation (28) with the line PS_1 is described by B_1. This can be interpreted in a similar manner as described in the previous section with the SISO system.

Manipulating equation (25) yields the alternative relation

$$r_e/r_{g1} = r_e/r_{g2} = r_{g1}/r_{g2} = r_{f1}/r_{h11} = r_{f1}/r_{h12} = r_{h11}/r_{h12} = 1, \quad a_1 \neq 1.$$

This is an equivalent relation describing the locus of detection and observation points relative to the locations of the primary source and secondary source one as the IGC circle. Thus, the situation can alternatively be interpreted as when the ratio of the distances from the primary source to the detection point and each observation point as well as to the pair of observation points and from secondary source one to the detection point and each observation point as well as to the pair of observation points are each equal to unity then the locus of detection and observation points is given by the IGC circle.

The loci given by the remaining two relations in equations (23) can be obtained through a similar analysis as above. Hence, the locus of detection and observation points leading to the IGC requirement are given in the second relation with respect to the locations of the primary source and secondary source two (say) and in the third relation with respect to the locations of the two secondary sources. In each case, as above, the locus, for unity distance ratio, is defined by a plane surface perpendicularly bisecting the line joining the locations of the two sources and, for a non-unity distance ratio, is defined by a circle with centre along the line joining the locations of the two sources and on a plane that is at right angles with this line. For the primary source and the secondary source located at points P and S_i $(i = 1, 2)$ respectively, the radius r_{ci} of the IGC circle corresponding to the first two relations in equation (23) is given by

$$r_{ci} = r_e \sin \theta_i, \quad 0 \leqslant \theta_i \leqslant \pi,$$

where, upon assuming the detector is located at point E in the medium, θ_i is the angle between lines PE and PS_i in a plane formed by these lines. The radius r_{c12} of the IGC circle corresponding to the third relation in equation (23), for the two secondary sources located at points S_1 and S_2 respectively, is given by

$$r_{c12} = r_{f1} \sin \theta_{12}, \quad 0 \leqslant \theta_{12} \leqslant \pi,$$

where, upon assuming the detector is located at point E, θ_{12} is the angle between the lines S_1E and S_1S_2.

By using the above analysis a generalization of the solution of equation (5) for an SIMO ANC system with k secondary sources can be obtained easily. It, thus, follows that in an SIMO ANC system the locus of detection and observation points leading to the IGC requirement is defined in relation to the locations of the primary source considered with each secondary source as well as each secondary source considered with any other secondary source. In this manner, for a system with k secondary sources a total of $\sum_{i=1}^{k} i$ pairs of sources can be identified. Among these, the primary source considered with each secondary source leads to k pairs, whereas the remaining $\sum_{i=1}^{k-1} i$ pairs are formed by considering the secondary sources with one another. In each case, assuming the two sources in question are located at points X and Y, the following two situations lead to the IGC requirement.

(a) When the detector and all observers are equidistant from points X and Y: this defines the locus of detection and observation points as a plane (the IGC plane) that perpendicularly bisects the line XY.

(b) When the distance ratios from point X to the detector and observer m ($m = 1, 2, \dots, k$) and to each pair of observation points as well as the distance ratios from point Y to the detector and observer m ($m = 1, 2, \dots, k$) and to each pair of observation points are each equal to unity: this defines the locus of detection and observation points as a circle (the IGC circle), with centre along a straight line passing through points X and Y, on a plane that is at right angles with this line.

Note that in an FBCS, where both the detection and observation points coincide with one another, the situation described in (a) above corresponds to the detection point being on the IGC plane. In an FFCS, however, this corresponds to the situation when the detection point and all the observation points are on the IGC plane. With the situation described in (b), on the other hand, an FBCS always satisfies the requirement. In an FFCS, however, it is possible to minimize the region of space occupied by the IGC circle by a proper geometrical arrangement of system components.

4.3. MULTI-INPUT MULTI-OUTPUT SYSTEM

Let the ANC system in Figure 1 incorporate n primary sources and k secondary sources. Thus, the controller transfer characteristics, $\mathbf{C}$, in equation (3) will represent an $n \times k$ matrix given by

$$\mathbf{C} = \begin{bmatrix} \mathbf{c}_{11} & \mathbf{c}_{12} & \cdots & \mathbf{c}_{1k} \\ \mathbf{c}_{21} & \mathbf{c}_{22} & \cdots & \mathbf{c}_{2k} \\ \cdots & \cdots & \cdots & \cdots \\ \mathbf{c}_{n1} & \mathbf{c}_{n2} & \cdots & \mathbf{c}_{nk} \end{bmatrix},$$

where $\mathbf{c}_{im}$ ($i = 1, 2, \dots, n$; $m = 1, 2, \dots, k$) represents the controller transfer function along the secondary path from detector i to secondary source m. In this manner, the controller is realized in an MIMO form as shown in Figure 4. Let the functions $\mathbf{E}(\mathrm{j}\omega)$, $\mathbf{F}(\mathrm{j}\omega)$, $\mathbf{G}(\mathrm{j}\omega)$ and $\mathbf{H}(\mathrm{j}\omega)$, thus, be represented as

$$\mathbf{E}(\mathrm{j}\omega) = \begin{bmatrix} \mathbf{e}_{11}(\mathrm{j}\omega) & \mathbf{e}_{12}(\mathrm{j}\omega) & \cdots & \mathbf{e}_{1n}(\mathrm{j}\omega) \\ \mathbf{e}_{21}(\mathrm{j}\omega) & \mathbf{e}_{22}(\mathrm{j}\omega) & \cdots & \mathbf{e}_{2n}(\mathrm{j}\omega) \\ \cdots & \cdots & \cdots & \cdots \\ \mathbf{e}_{n1}(\mathrm{j}\omega) & \mathbf{e}_{n2}(\mathrm{j}\omega) & \cdots & \mathbf{e}_{nn}(\mathrm{j}\omega) \end{bmatrix}, \tag{29a}$$

$$\mathbf{F}(\mathrm{j}\omega) = \begin{bmatrix} \mathbf{f}_{11}(\mathrm{j}\omega) & \mathbf{f}_{12}(\mathrm{j}\omega) & \cdots & \mathbf{f}_{1n}(\mathrm{j}\omega) \\ \mathbf{f}_{21}(\mathrm{j}\omega) & \mathbf{f}_{22}(\mathrm{j}\omega) & \cdots & \mathbf{f}_{2n}(\mathrm{j}\omega) \\ \cdots & \cdots & \cdots & \cdots \\ \mathbf{f}_{k1}(\mathrm{j}\omega) & \mathbf{f}_{k2}(\mathrm{j}\omega) & \cdots & \mathbf{f}_{kn}(\mathrm{j}\omega) \end{bmatrix}, \tag{29b}$$

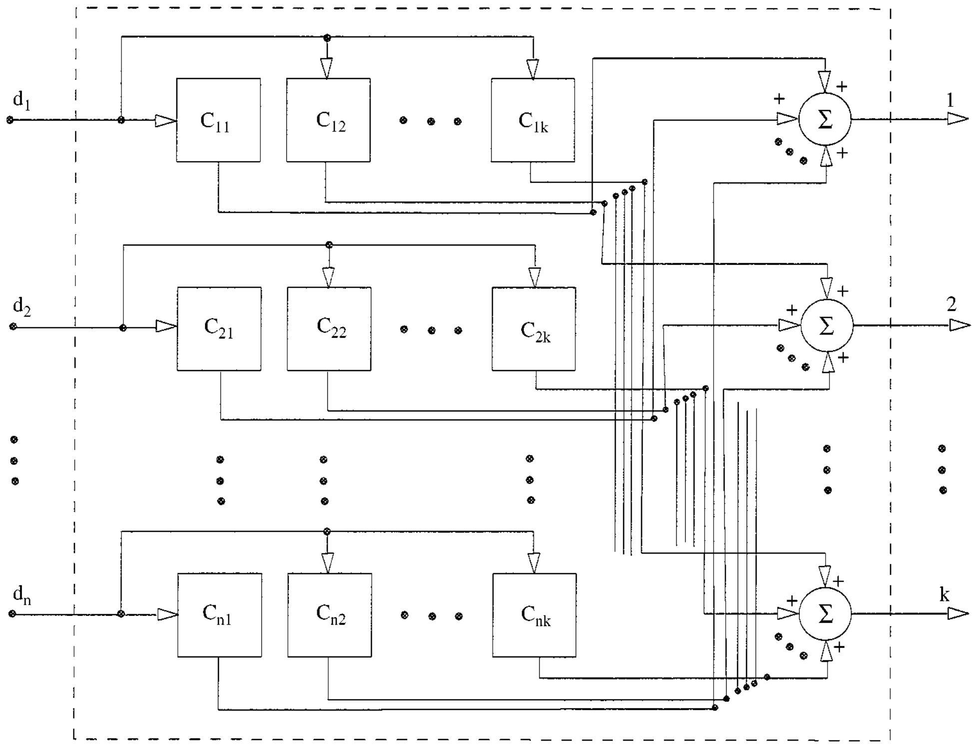

Figure 4. MIMO controller.

$$\mathbf{G}(j\omega) = \begin{bmatrix} \mathbf{g}_{11}(j\omega) & \mathbf{g}_{12}(j\omega) & \cdots & \mathbf{g}_{1k}(j\omega) \\ \mathbf{g}_{21}(j\omega) & \mathbf{g}_{22}(j\omega) & \cdots & \mathbf{g}_{2k}(j\omega) \\ \cdots & \cdots & \cdots & \cdots \\ \mathbf{g}_{n1}(j\omega) & \mathbf{g}_{n2}(j\omega) & \cdots & \mathbf{g}_{nk}(j) \end{bmatrix}, \tag{29c}$$

$$\mathbf{H}(j\omega) = \begin{bmatrix} \mathbf{h}_{11}(j\omega) & \mathbf{h}_{12}(j\omega) & \cdots & \mathbf{h}_{1k}(j\omega) \\ \mathbf{h}_{21}(j\omega) & \mathbf{h}_{22}(j\omega) & \cdots & \mathbf{h}_{2k}(j\omega) \\ \cdots & \cdots & \cdots & \cdots \\ \mathbf{h}_{k1}(j\omega) & \mathbf{h}_{k2}(j\omega) & \cdots & \mathbf{h}_{kk}(j\omega) \end{bmatrix}, \tag{29d}$$

where

$$\mathbf{e}_{im}(j\omega) = \frac{A}{r_{eim}} e^{-j(\omega/c)r_{eim}}, \quad \mathbf{f}_{sm}(j\omega) = \frac{A}{r_{fsm}} e^{-j(\omega/c)r_{fsm}}$$

$$\mathbf{g}_{is}(j\omega) = \frac{A}{r_{gis}} e^{-j(\omega/c)r_{gis}}, \quad \mathbf{h}_{st}(j\omega) = \frac{A}{r_{hst}} e^{-j(\omega/c)r_{hst}}, \tag{30}$$

$i = 1, 2, \ldots, n$, $m = 1, 2, \ldots, n$, $s = 1, 2, \ldots, k$, $t = 1, 2, \ldots, k$, A is a constant and $r_{eim}, r_{fsm}, r_{gis}$ and r_{hst} are the distances of the acoustic paths with transfer characteristics $\mathbf{e}_{im}(j\omega)$, $\mathbf{f}_{sm}(j\omega)$, $\mathbf{g}_{is}(j\omega)$ and $\mathbf{h}_{st}(j\omega)$ respectively. Substituting for $\mathbf{E}(j\omega)$, $\mathbf{F}(j\omega)$, $\mathbf{G}(j\omega)$ and $\mathbf{H}(j\omega)$ from equation (29) into equation (5) and manipulating yields the set of solutions

$$\frac{\mathbf{e}_{i1}}{\mathbf{e}_{m1}}=\frac{\mathbf{e}_{i2}}{\mathbf{e}_{m2}}=\cdots=\frac{\mathbf{e}_{in}}{\mathbf{e}_{mn}}=\frac{\mathbf{g}_{i1}}{\mathbf{g}_{m1}}=\frac{\mathbf{g}_{i2}}{\mathbf{g}_{m2}}=\cdots=\frac{\mathbf{g}_{ik}}{\mathbf{g}_{mk}},$$
$$i=1,2,\dots,n,\quad m=1,2,\dots,n,\quad i\neq m, \tag{31a}$$

$$\frac{\mathbf{f}_{i1}}{\mathbf{e}_{m1}}=\frac{\mathbf{f}_{i2}}{\mathbf{e}_{m2}}=\cdots=\frac{\mathbf{f}_{ik}}{\mathbf{e}_{mn}}=\frac{\mathbf{h}_{i1}}{\mathbf{g}_{m1}}=\frac{\mathbf{h}_{i2}}{\mathbf{g}_{m2}}=\cdots=\frac{\mathbf{h}_{ik}}{\mathbf{g}_{mk}},$$
$$i=1,2,\dots,k,\quad m=1,2,\dots,n, \tag{31b}$$

$$\frac{\mathbf{f}_{i1}}{\mathbf{f}_{m1}}=\frac{\mathbf{f}_{i2}}{\mathbf{f}_{m2}}=\cdots=\frac{\mathbf{f}_{in}}{\mathbf{f}_{mn}}=\frac{\mathbf{h}_{i1}}{\mathbf{h}_{m1}}=\frac{\mathbf{h}_{i2}}{\mathbf{h}_{m2}}=\cdots=\frac{\mathbf{h}_{ik}}{\mathbf{h}_{mk}},$$
$$i=1,2,\dots,k,\quad m=1,2,\dots,k,\quad i\neq m. \tag{31c}$$

Substituting for the functions in equation (31) from equation (30) accordingly and simplifying yields

$$\frac{r_{em1}}{r_{ei1}}=\frac{r_{em2}}{r_{ei2}}=\cdots=\frac{r_{emn}}{r_{ein}}=\frac{r_{gm1}}{r_{gi1}}=\frac{r_{gm2}}{r_{gi2}}=\cdots=\frac{r_{gmk}}{r_{gik}}=a_p,$$
$$r_{ei1}-r_{em1}=r_{ei2}-r_{em2}=\cdots=r_{ein}-r_{emn}=r_{gi1}-r_{gm1}$$
$$=r_{gi2}-r_{gm2}=\cdots=r_{gik}-r_{gmk},$$
$$i=1,2,\dots,n,\quad m=1,2,\dots,n,\quad i\neq m, \tag{32a}$$

$$\frac{r_{em1}}{r_{fi1}}=\frac{r_{em2}}{r_{fi2}}=\cdots=\frac{r_{emn}}{r_{fin}}=\frac{r_{gm1}}{r_{hi1}}=\frac{r_{gm2}}{r_{hi2}}=\cdots=\frac{r_{gmk}}{r_{hik}}=a_{ps},$$
$$r_{fi1}-r_{em1}=r_{fi2}-r_{em2}=\cdots=r_{fin}-r_{emn}=r_{hi1}-r_{gm1}$$
$$=r_{hi2}-r_{gm2}-r_{gm2}=\cdots=r_{hik}-r_{gmk},$$
$$i=1,2,\dots,k,\quad m=1,2,\dots,n, \tag{32b}$$

$$\frac{r_{fm1}}{r_{fi1}}=\frac{r_{fm2}}{r_{fi2}}=\cdots=\frac{r_{fmn}}{r_{fin}}=\frac{r_{hm1}}{r_{hi1}}=\frac{r_{hm2}}{r_{hi2}}=\cdots=\frac{r_{hmk}}{r_{hik}}=a_s,$$
$$r_{fi1}-r_{fm1}=r_{fi2}-r_{fm2}=\cdots=r_{fin}-r_{fmn}$$
$$=r_{hi1}-r_{hm1}=r_{hi2}-r_{hm2}=\cdots=r_{hik}-r_{hmk},$$
$$i=1,2,\dots,k,\quad m=1,2,\dots,k,\quad i\neq m, \tag{32c}$$

where a_p, a_{ps} and a_s are positive real numbers representing distance ratios. Equations (32) define loci of detection and observation points relative to the locations of the sources in the medium for which the IGC requirement holds. In particular, equation (32a) defines the locus of detection and observation points relative to the locations of primary sources i and m, equation (32b) defines the locus with respect to the locations of primary source m and secondary source i and equation (32c) defines the locus with respect to the locations of secondary sources i and m. It follows from Appendix A and the analysis presented in the previous sections that, in each case, assuming the two sources in question are located at points X and Y respectively, the locus for the corresponding distance ratio being unity is a plane perpendicularly bisecting the line XY. For a non-unity distance ratio, however, the locus is a circle, with centre along a line passing through the points X and Y, in a plane that is at right angles with this line.

It follows from the above that in an MIMO ANC system the locus of detection and observation points leading to the IGC requirement is defined in relation to the locations of all possible pairs of sources, each pair considered at a time. In this manner, for a system with n primary sources and k secondary sources a total of $\sum_{i=1}^{k-1} i + \sum_{m=1}^{n-1} m + nk$ pairs of sources can be identified. Among these, the primary sources considered with one another lead to $\sum_{m=1}^{n-1} m$ pairs, the secondary sources considered with one another lead to $\sum_{i=1}^{k-1} i$ pairs and the remaining nk pairs are formed by considering each primary source with the secondary sources. In each case, assuming the two sources in question are located at points X and Y, the following two situations lead to the IGC requirement.

(a) When all the detectors and observers are equidistant from points X and Y. This defines the locus of detection and observation points as a plane (the IGC plane) that perpendicularly bisects the line XY.

(b) When the distance ratios from point X to each pair of detection points, to detector i ($i = 1, 2, \ldots, n$) and observer m ($m = 1, 2, \ldots, k$) and to each pair of observation points as well as the distance ratios from point Y to each pair of detection points, to detector i ($i = 1, 2, \ldots, n$) and observer m ($m = 1, 2, \ldots, k$) and to each pair of observation points are each equal to unity. This defines the locus of detection and observation points as a circle (the IGC circle), with centre along a line passing through points X and Y, on a plane that is at right angles with this line.

Note that in an FBCS, where both the detection and observation points coincide with one another, the situation described in (a) above corresponds to the detection points being on the IGC plane. In an FFCS, however, this corresponds to the situation when all the detection and observation points are on the IGC plane. With the situation described in (b), on the other hand, an FBCS always satisfies the requirement. In an FFCS, however, it is possible to minimize the region of space occupied by the IGC circle by a proper geometrical arrangement of system components.

The analysis presented in the preceding sections corresponds to ANC systems in a three-dimensional free-field propagation medium. This is carried out by utilizing a standard characterization of sound radiation in the medium as given in terms of distance from a radiating point source. The analysis can be extended to one-dimensional and three-dimensional enclosed sound fields through the utilization of a similar characterization of sound radiation in these media in terms of distances accordingly.

The conditions for the IGC requirement obtained above correspond to the general ANC structure in Figure 1 for optimum cancellation of noise at the observation points. For a control structure with sub-optimal performance, similar conditions can be reached at by setting a performance criterion based on which the controller can be designed and interpreted in terms of transfer characteristics of the acoustic paths in the propagation medium. Such an interpretation can then easily lead to an analysis similar to that presented above and the corresponding constraints in the geometrical arrangement of system components.

5. CONCLUSION

An analysis and design procedure for ANC systems in a three-dimensional non-dispersive propagation medium on the basis of optimum cancellation of noise has been presented. The relation between the transfer characteristics of the required controller and the geometrical arrangement of system components has been studied and conditions interpreted as geometrical constraints in the design of ANC systems have been derived and analyzed.

For optimum cancellation of noise to be achieved at the observation points in the medium the controller is required to have suitable continuous frequency-dependent characteristics to produce a cancelling wave that is an exact mirror image of the noise. The transfer characteristics of such a controller are found to be dependent upon the transfer characteristics of transducers, secondary sources and propagation paths from the primary and secondary sources to the detection and observation points.

The dependence of controller characteristics on the acoustic paths in the system, arising from geometrical arrangement of system components, can sometimes lead to practical difficulties in the design of the controller and to instability problems in the system. A particular arrangement of system components requires the controller to have particular transfer characteristics. In particular, there are specific arrangements of system components, identified as loci of detection and observation points relative to the sources, which lead to the critical situation of the IGC requirement. In an SISO ANC structure, two situations are found, in general, that lead to the IGC requirement.

(i) When both the observer and detector are equidistant from the primary and secondary sources. This corresponds to the locus of detection and observation points forming a plane that perpendicularly bisects the line joining the locations of the sources.

(ii) When the ratio of the distances from the primary source to the detector and observer and the ratio of the distances from the secondary source to the detector and observer are each equal to unity. This corresponds to the locus of detection and observation points forming a circle, with centre along a straight line passing through the locations of the primary and secondary sources, in a plane that is at right angles with this line.

In an SIMO ANC structure, the locus of detection and observation points leading to the IGC requirement is defined in relation to the locations of the primary source considered with each secondary source as well as each secondary source considered with any other secondary source. In each case, assuming the two sources in question are located at points X and Y, the following two situations lead to the IGC requirement

(iii) When the detector and all observors are equidistant from points X and Y. This defines the locus of detection and observation points as a plane that perpendicularly bisects the line XY.

(iv) When the distance ratios from point X to the detector and observer m ($m = 1, 2, \dots, k$) and to each pair of observation points as well as the distance ratios from point Y to the detector and observer m ($m = 1, 2, \dots, k$) and to each pair of observation points are each equal to unity. This defines the locus of detection and observation points as a circle, with centre along a straight line passing through points X and Y, on a plane that is at right angles with this line.

In an MIMO ANC structure the locus of detection and observation points leading to the IGC requirement is defined in relation to the locations of all possible pairs of sources, each pair considered at a time. In each case, assuming the two sources in question are located at points X and Y, the following two situations lead to the IGC requirement

(v) When all the detectors and observers are equidistant from points X and Y. This defines the locus of detection and observation points as a plane that perpendicularly bisects the line XY.

(vi) When the distance ratios from point X to each pair of detection points, to detector i ($i = 1, 2, \dots, n$) and observer m ($m = 1, 2, \dots, k$) and to each pair of observation points as well as the distance ratios from point Y to each pair of detection points, to detector i ($i = 1, 2, \dots, n$) and observer m ($m = 1, 2, \dots, k$) and to each pair of observation points are each equal to unity. This defines the locus of detection and observation points as a circle, with centre along a straight line passing through points X and Y, on a plane that is at right angles with this line.

In an FBCS, where both the detection and observation points coincide with one another, the situation leading to the IGC plane corresponds to the detection point(s) being on the IGC plane. In an FFCS, however, this corresponds to the situation when the detection as well as the observation points are on the IGC plane. With the situation leading to the IGC circle, on the other hand, an FBCS always satisfies the requirement. In an FFCS, however, it is possible to minimize the region of space occupied by the IGC circle by a proper geometrical arrangement of system components.

REFERENCES

1. R. R. Leitch and M. O. Tokhi 1987 *IEE Proceedings-A* **134**, 525–546. Active noise control systems.
2. M. O. Tokhi and R. R. Leitch 1992 *Active Noise Control*. Oxford: Clarendon Press.
3. P. A. Nelson and S. J. Elliott 1992 *Active Control of Sound*. London: Academic Press.
4. R. R. Leitch and M. O. Tokhi 1986 *Proceedings of the Institute of Acoustics* **8** (Part 1), 149–157. The implementatin of active noise control systems using digital signal processing techniques.

5. W. B. Conover 1956 *Noise Control* **92**, 78–82 & 92. Fighting noise with noise.
6. W. B. Conover 1957 *US Patent No. 2 776 020. Noise reducing system for transformers.*
7. B. Chaplin 1980 *Proceedings of Inter-noise 80: International Conference on Noise Control Engineering, FL, 8–10 December 1980* **II**, 699–702. The cancellation of repetitive noise and vibration.
8. J. C. Burgess 1981 *Journal of the Acoustical Society of America* **70**, 715–726. Active adaptive sound control in a duct: a computer simulation.
9. C. F. Ross 1982 *Journal of Sound and Vibration* **80**, 381–388. An adaptive digital filter for broadband active sound control.
10. A. M. Alvarez-Tinoco 1985 *PhD. Thesis, Heriot-Watt University, Department of Electrical and Electronic Engineering, Edinburgh, UK*. Adaptive algorithms for the active attenuation of acoustic noise.
11. P. Darlington and S. J. Elliott 1985 *Proceedings of the Institute of Aoustics* **7** (Part 2), 87–94. Adaptive control of periodic disturbances in resonant systems.
12. S. J. Elliott and P. A. Nelson 1986 *Proceedings of the Institute of Acoustics* **8** (Part 1), 135–147. An adaptive algorithm for multichannel active control.
13. S. J. Elliott, I. M. Sothers and P. A. Nelson 1987 *IEEE Transactions on Acoustics, Speech, and Signal Processing* **ASSP-35**, 1423–1434. A multiple error LMS algorithm and its application to the active control of sound and vibration.
14. L. J. Eriksson, M. C. Allie and R. A. Greiner 1987 *IEEE Transactions on Acoustics, Speech, and Signal Processing* **ASSP-35**, 433–437. The selection and application of an IIR adaptive filter for use in active sound attenuation.
15. L. J. Eriksson, M. C. Allie, C. D. Bremigan and R. A. Greiner 1988 *Proceedings of the IEEE International Conference on Acoustics, Speech, and Signal Processing, New York*, **5**, 2594–2597. Active noise control using adaptive digital signal processing.
16. M. O. Tokhi and R. R. Leitch 1989 *IEE Digest No. 1989/46: Colloquium on Adaptive Filters, London, 22 March 1989*, 91/1–91/4. Self-tuning active noise control.
17. M. O. Tokhi and R. R. Leitch 1991 *IEE Proceedings-D* **138**, 421–430. Design and implementation of self-tuning active noise control systems.
18. M. Jessel and G. A. Mangiante 1972 *Journal of Sound and Vibration* **23**, 383–390. Active sound absorbers in an air duct.
19. M. A. Swinbanks 1973 *Journal of Sound and Vibration* **27**, 411–436. Active control of sound propagation in long ducts.
20. H. G. Leventhall 1976 *Proceedings of Noise Control Conference, Warsaw*, 13–15 October 1976, 33–42. Developments in active attenuators.
21. H. G. Leventhal and Kh. Eghtesadi 1979 *Proceedings of Inter-noise 79: International Conference on Noise Control Engineering, Warsaw* 11–13 September 1979 **I**, 175–180. Active attenuation of noise: monopole and dipole systems.
22. Kh. Eghtesadi and H. G. Leventhal 1981 *Acoustics Letters* **4**, 204–209. Comparison of active attenuators of noise in ducts.
23. M. O. Tokhi and R. R. Leitch 1991 *Noise Control Engineering Journal* **36**, 41–53. Design of active noise control systems operating in three-dimensional dispersive propagation medium.
24. M. O. Tokhi and R. R. Leitch 1991 *Journal of the Acoustical Society of America* **90**, 334–345. The robust design of active noise control systems based on relative stability measures.
25. P. Lueg 1936 *US Patent No. 2 043 416.* Process of silencing sound oscillations.
26. M. O. Tokhi and R. R. Leitch 1988 *Proceedings of Inter-noise 88: International Conference on Noise Control Engineering, Avignon* 30 August – 01 September 1988 **2**, 1037–1040. Practical limitations in the controller design for active noise control systems in three-dimensions.
27. H. F. Olson and E. G. May 1953 *Journal of the Acoustical Society of America* **25**, 1130–1136. Electronic sound absorbers.

28. H. F. OLSON 1956 *Journal of the Acoustical Society of America* **28**, 966–972. Electronic control of noise, vibration and reverberation.
29. H. F. OLSON 1961 *US Patent No. 2 983 790*. Electronic sound absorber.
30. J. C. BLEZAY 1962 *Journal of the Audio Eningeering Society* **10**, 135–139. Electronic sound absorber.
31. W. R. SHORT 1980 *Proceedings of Inter-noise* 80: *International Conference on Noise Control Engineering*, *Florida*, 8–10 *December* 1980 **II**, 695–698. Global low frequency active noise attenuation.
32. M. C. J. TRINDER and P. A. NELSON 1983 *Proceedings of Inter-noise* 83: *International Conference on Noise Control Engineering*, *Edinburgh*, 13–15 *July* 1983, **I**, 447–450. The acoustical virtual earth and its application to ducts with reflecting terminations.
33. M. C. J. TRINDER and P. A. NELSON 1983 *Journal of Sound and Vibration* **89**, 95–106. Active noise control in finite length ducts.
34. G. B. B. CHAPLIN, A. JONES and O. JONES 1985 *US Patent No. 4 527 282*. Method and apparatus for low frequency active attenuation.
35. A. ROURE 1985 *Journal of Sound and Vibration* **101**, 429–441. Self-adaptive broadband active sound control system.
36. N. HESSELMAN 1978 *Applied Acoustics* **11**, 27–34. Investigation of noise reduction on a 100 KVA transformer tank by means of active methods.
37. C. F. ROSS 1978 *Journal of Sound and Vibration* **61**, 473–480. Experiments on the active control of transformer noise.
38. M. L. MUNJAL and L. J. ERIKSSON 1988 *Journal of the Acoustical Society of America* **84**, 1086–1093. An analytical, one-dimensional, standing-wave model of a linear active noise control system in a duct.
39. P. A. NELSON, A. R. D. CURTIS, S. J. ELLIOTT and A. J. BULLMORE 1987 *Journal of Sound and Vibration* **117**, 1–13. The acitve minimization of harmonic enclosed sound fields, Part I: theory.

APPENDIX A: LOCUS OF CONSTANT DISTANCE RATIO

Consider two fixed points $P(0, 0, 0)$ and $S(u_s, v_s, w_s)$ and an arbitrary point $T(u, v, w)$ in a three-dimensional UVW-space. Let the distances PS, PT and ST be denoted by r, r_g and r_h respectively:

$$r = \sqrt{u_s^2 + v_s^2 + w_s^2}\,, r_g = \sqrt{u^2 + v^2 + w^2}\,, r_h = \sqrt{(u - u_s) + (v - v_s)^2 + (w - w_s)^2}\,, \tag{A1}$$

Let the distance ratio r_g/r_h be denoted by, a positive real number, a:

$$r_g/r_h = a. \tag{A2}$$

Substituting for r_g and r_h from equation (A1) into equation (A2), simplifying and using equation (A1) yields

$$(1 - a^2)u^2 + 2a^2u_su + (1 - a^2)v^2 + 2a^2v_sv + (1 - a^2)w^2 + 2a^2w_sw = a^2d^2. \tag{A3}$$

This gives the locus of points in the UVW-space that corresponds to a particular distance ratio a.

A.1. NON-UNITY DISTANCE RATIO

If the distance ratio a is not unity then equation (A3), after completing squares and simplifying, yields

$$\left[u+\frac{a^2u_s}{1-a^2}\right]^2+\left[v+\frac{a^2v_s}{1-a^2}\right]^2+\left[w+\frac{a^2w_s}{1-a^2}\right]^2=\left[\frac{ar}{1-a^2}\right]^2, \quad a\neq 1, \tag{A4}$$

This represents a sphere with radius $R = ar/|1-a^2|$ and centre at $Q(-a^2u_s/(1-a^2),\ -a^2v_s/(1-a^2), a^2w_s/(1-a^2))$.

To obtain the location of the centre of the sphere Q in relation to points P and S, let the coordinates of point Q be denoted by (u_q, v_q, w_q), unit vectors in the directions of $U-$, $V-$ and $W-$ axes be denoted by i, j and k respectively and unit vectors along lines PS and PQ pointing towards points S and Q respectively be denoted by I_{ps} and I_{pq}:

$$u_q=-\frac{a^2u_s}{1-a^2}, \quad v_q=-\frac{a^2v_s}{1-a^2}, \quad w_q=-\frac{a^2w_s}{1-a^2}, \tag{A5}$$

$$I_{ps}=\frac{u_si+v_sj+w_sk}{\sqrt{u_s^2+v_s^2+w_s^2}}, \quad I_{pq}=\frac{u_qi+v_qj+w_qk}{\sqrt{u_q^2+v_q^2+w_q^2}}. \tag{A6}$$

Substituting for u_q, v_q and w_q from equation (A5) into equation (A6), simplifying and using equation (A1) yields

$$I_{ps}=\frac{1}{r}(u_si+v_sj+w_sk), \quad I_{pq}=-\frac{|1-a^2|}{1-a^2}\frac{1}{r}(u_si+v_sj+w_sk), \tag{A7}$$

or

$$I_{pq}=\begin{cases} +I_{ps} & \text{for } a>1, \\ -I_{ps} & \text{for } a<1. \end{cases} \tag{A8}$$

It follows from equation (A8) that the centre of the sphere (point Q) is located along the line PS and, specifically, if P is chosen as reference then for $a>1$ the centre is located on the portion of PS corresponding to points away from P in the direction of I_{ps}, whereas for $a<1$ the centre of the sphere will be on the portion of PS corresponding to points away from P in the direction of $-I_{ps}$. In either of these situations, as follows from equation (A5), the centre of the sphere lies outside the range (P, S). This is shown below.

Let the distance between points P and Q be denoted by r_{pq} and the distance between points Q and S be denoted by r_{sq}:

$$r_{pq}=\sqrt{u_q^2+v_q^2+w_q^2}, \quad r_{sq}=\sqrt{(u_q-u_s)^2+(v_q-v_s)^2+(w_q+w_s)^2}.$$

Substituting for u_q, v_q and w_q from equation (A5) into the above, using equation (A1) and simplifying yields

$$r_{pq}=a^2r/|1-a^2|, \quad r_{sq}=r/|1-a^2|,$$

which implies that

$$r_{pq} > r_{sq} \text{ and } r_{pq} > r \text{ for } a > 1, \; r_{pq} < r_{sq} \text{ and } r_{sq} > r \text{ for } a < 1.$$

Therefore, point Q is always outside the range (P, S).

Let the line passing through points P and S intersect the sphere in equation (A4) at point $N(u_n, v_n, w_n)$ with distances r_{pn} and r_{sn} relative to points P and S respectively and let the unit vectors pointing towards N from points P and S be denoted by I_{pn} and I_{sn} respectively:

$$r_{pn} = \sqrt{u_n^2 + v_n^2 + w_n^2}, \quad r_{sn} = \sqrt{(u_n - u_s)^2 + (v_n - v_s)^2 + (w_n - w_s)^2}.$$

and

$$I_{pn} = \frac{u_n i + v_n j + w_n k}{r_{pn}}, \quad I_{sn} = \frac{(u_n - u_s)i + (v_n - v_s)j + (w_n + w_s)k}{r_{sn}}. \tag{A9}$$

Since N is a point along the line PS, the vectors I_{pn} and I_{sn} are pointing either in the same or in opposite directions. Therefore, it follows from equation (A9) that

$$\frac{|u_n|}{r_{pn}} = \frac{|u_n - u_s|}{r_{sn}}, \quad \frac{|v_n|}{r_{pn}} = \frac{|v_n - v_s|}{r_{sn}}, \quad \frac{|w_n|}{r_{pn}} = \frac{|w_n - w_s|}{r_{sn}}. \tag{A10}$$

Since r_{pn}/r_{sn} represents the distance ratio a, equation (A10) can be written as

$$u_n^2 = a^2(u_n - u_s)^2, \quad v_n^2 = a^2(v_n - v_s)^2, \quad w_n^2 = a^2(w_n - w_s)^2. \tag{A11}$$

Solving equation (A11) for u_n, v_n and w_n yields

$$u_n = \left(\frac{-a^2 \pm a}{1 - a^2}\right) u_s, \quad v_n = \left(\frac{-a^2 \pm a}{1 - a^2}\right) v_s, \quad w_n = \left(\frac{-a^2 \pm a}{1 - a^2}\right) w_s. \tag{A12}$$

It follows from equation (A12) that a line, passing through points P and S, and the sphere in equation (A4) intersect at two points E and F with co-ordinates (u_e, v_e, w_e) and (u_f, v_f, w_f) respectively:

$$u_e = \frac{a}{1 + a} u_s, \quad v_e = \frac{a}{1 + a} v_s, \quad w_e = \frac{a}{1 + a} w_s, \tag{A13}$$

$$u_f = -\frac{a}{1 - a} u_s, \quad v_f = -\frac{a}{1 - a} v_s, \quad w_f = -\frac{a}{1 - a} w_s. \tag{A14}$$

Equations (A13) and (A14) imply that point E is always located inside the range (P, S) and point F outside this range. In particular, if $a > 1$ then points E and F are closer to point S whereas if $a < 1$ then points E and F are closer to point P. If the distances from points E and F to points P and S are denoted respectively by r_{pe}. r_{se} and r_{pf}, r_{sf} then, upon using equations (A1), (A13) and (A14) these distances are given by

$$r_{pe} = \frac{ar}{1 + a}, \quad r_{se} = \frac{r}{1 + a}, \quad r_{pf} = \frac{ar}{|1 - a|}, \quad r_{sf} = \frac{r}{|1 - a|}.$$

A.2. UNITY DISTANCE RATIO

If the distance ratio a is unity, then equation (A2) yields

$$r_g = r_h. \tag{A15}$$

Substituting for r_g and r_h from equation (A1) into equation (A15), simplifying and using equation (A1) yields

$$\frac{u}{(r^2/2u_s)} + \frac{v}{(r^2/2v_s)} + \frac{w}{(r^2/2w_s)} = 1. \tag{A16}$$

This represents a plane surface which intersects the $U-$, $V-$ and $W-$ axes at points $(r^2/2u_s, 0, 0)$, $(0, r^2/2v_s, 0)$ and $(0, 0, r^2/2w_s)$ respectively.

The direction of the plane in equation (A16) is represented by a unit vector at right angles with the surface and pointing outward from the surface. Let such a unit vector be denoted by I_s. Simplifying equation (A16) yields

$$2u_s u + 2v_s v + 2w_s w - r^2 = 0.$$

Let the left-hand side of the above equation be denoted by a variable Z:

$$Z = 2u_s u + 2v_s v + 2w_s w - r^2. \tag{A17}$$

As Z varies from $-\infty$ to $+\infty$ equation (A17) defines an infinite set of plane surfaces parallel to the plane in equation (A16). Thus, the unit vector I_s is given by

$$I_s = \frac{(\partial Z/\partial u)\, i + (\partial Z/\partial v)\, j + (\partial Z/\partial w)\, k}{\sqrt{(\partial Z/\partial u)^2 + (\partial Z/\partial v)^2 + (\partial Z/\partial w)^2}}, \tag{A18}$$

where $\partial/\partial u$, $\partial/\partial v$ and $\partial/\partial w$ denote the partial derivatives with respect to u, v and w respectively. Substituting for Z from equation (A17) into equation (A18), simplifying and using equation (A1) yields

$$I_s = \frac{u_s}{r}\, i + \frac{v_s}{r}\, j + \frac{w_s}{r}\, k. \tag{A19}$$

Comparing equation (A19) with equation (A7) yields

$$I_s = I_{ps}. \tag{A20}$$

Equation (A20) implies that the line PS is perpendicular to the plane surface in equation (A16). Moreover, it follows from equation (A15) that the point of intersection of the plane and the line PS is equidistant from points P and S. Therefore, the plane in equation (A16) perpendicularly bisects the line PS.

In a two-dimensional space, the locus of constant distance ratio can be obtained through a similar manipulation as presented above and equivalent interpretations of the corresponding results can be made. In this manner, for a non-unity distance ratio, the locus is given by a circle with centre along the line PS. For a unity distance ratio, however, the locus is given by a straight line perpendicularly bisecting the line joining points P and S.